A&A 444, 327–336 (2005)
DOI: 10.1051/0004-6361:20052715

Astronomy & Astrophysics

Temperature and polarization angular power spectra of Galactic dust radiation at 353 GHz as measured by Archeops

N. Ponthieu[1,2], J. F. Macías-Pérez[2], M. Tristram[2], P. Ade[3], A. Amblard[4], R. Ansari[5], J. Aumont[2], É. Aubourg[6,7], A. Benoît[8], J.-Ph. Bernard[9], A. Blanchard[10], J. J. Bock[11,12], F. R. Bouchet[13], A. Bourrachot[5], P. Camus[8], J.-F. Cardoso[14,7], F. Couchot[5], P. de Bernardis[15], J. Delabrouille[14,7], F.-X. Désert[16], M. Douspis[10], L. Dumoulin[17], Ph. Filliatre[18], P. Fosalba[19], M. Giard[9], Y. Giraud-Héraud[14,7], R. Gispert[1,†,⋆], J. Grain[2], L. Guglielmi[14,7], J.-Ch. Hamilton[20], S. Hanany[21], S. Henrot-Versillé[5], J. Kaplan[14,7], G. Lagache[1], A. E. Lange[12], K. Madet[8], B. Maffei[3], S. Masi[15], F. Mayet[2], F. Nati[15], G. Patanchon[22], O. Perdereau[5], S. Plaszczynski[5], M. Piat[14,7], S. Prunet[13], J.-L. Puget[1], C. Renault[2], C. Rosset[14,7], D. Santos[2], D. Vibert[13], and D. Yvon[6,7]

[1] Institut d'Astrophysique Spatiale, Bât. 121, Université Paris XI, 91405 Orsay Cedex, France
e-mail: reprints@archeops.org
[2] Laboratoire de Physique Subatomique et de Cosmologie, 53 avenue des Martyrs, 38026 Grenoble Cedex, France
e-mail: macias@in2p3.fr
[3] Cardiff University, Physics Department, PO Box 913, 5, The Parade, Cardiff, CF24 3YB, UK
[4] University of California, Berkeley, Dept. of Astronomy, 601 Campbell Hall, Berkeley, CA 94720-3411, USA
[5] Laboratoire de l'Accélérateur Linéaire, BP 34, Campus Orsay, 91898 Orsay Cedex, France
[6] CEA-CE Saclay, DAPNIA, Service de Physique des Particules, Bât 141, 91191 Gif-sur-Yvette Cedex, France
[7] Fédération de Recherche APC, Université Paris 7, Paris, France
[8] Centre de Recherche sur les Très Basses Températures, BP166, 38042 Grenoble Cedex 9, France
[9] Centre d'Étude Spatiale des Rayonnements, BP 4346, 31028 Toulouse Cedex 4, France
[10] Laboratoire d'Astrophysique de Tarbes Toulouse, OMP, UPS, CNRS UMR 5572, 14 Av. E. Belin 31400 Toulouse, France
[11] California Institute of Technology, 105-24 Caltech, 1201 East California Blvd, Pasadena CA 91125, USA
[12] Jet Propulsion Laboratory, 4800 Oak Grove Drive, Pasadena, California 91109, USA
[13] Institut d'Astrophysique de Paris, 98bis boulevard Arago, 75014 Paris, France
[14] Physique Corpusculaire et Cosmologie, Collège de France, 11 Pl. M. Berthelot, 75231 Paris Cedex 5, France
[15] Gruppo di Cosmologia Sperimentale, Dipart. di Fisica, Univ. "La Sapienza", P. A. Moro, 2, 00185 Roma, Italy
[16] Laboratoire d'Astrophysique, Obs. de Grenoble, BP 53, 38041 Grenoble Cedex 9, France
[17] CSNSM-IN2P3, Bât 108, 91405 Orsay Campus, France
[18] CEA-CE Saclay, DAPNIA, Service d'Astrophysique, Bât 709, 91191 Gif-sur-Yvette Cedex, France
[19] Institute for Astronomy, University of Hawaii, 2680 Woodlawn Dr, Honolulu, HI 96822, USA
[20] LPNHE, Universités Paris VI et Paris VII, 4 place Jussieu, Tour 33, 75252 Paris Cedex 05, France
[21] School of Physics and Astronomy, 116 Church St. S.E., University of Minnesota, Minneapolis MN 55455, USA
[22] Department of Physics & Astronomy, University of British Columbia, 6224 Agricultural Road, Vancouver, BC V6T 1Z1, Canada

Received 21 January 2005 / Accepted 11 August 2005

ABSTRACT

We present the first measurement of temperature and polarization angular power spectra of the diffuse emission of Galactic dust at 353 GHz as seen by Archeops on 20% of the sky. The temperature angular power spectrum is compatible with that provided by the extrapolation to 353 GHz of IRAS and DIRBE maps using Finkbeiner et al. (1999, ApJ, 524, 867) model number 8. For Galactic latitudes $|b| \geq 5$ deg we report a 4 sigma detection of large scale ($3 \leq \ell \leq 8$) temperature-polarization cross-correlation $(\ell+1)C_\ell^{TE}/2\pi = 76 \pm 21\ \mu\mathrm{K}^2_{\mathrm{RJ}}$ and set upper limits to the E and B mode polarization at 11 $\mu\mathrm{K}^2_{\mathrm{RJ}}$. For Galactic latitudes $|b| \geq 10$ deg, on the same angular scales, we report a 2 sigma detection of temperature-polarization cross-correlation $(\ell+1)C_\ell^{TE}/2\pi = 24 \pm 13\ \mu\mathrm{K}^2_{\mathrm{RJ}}$. These results are then extrapolated to 100 GHz to estimate the contamination in CMB measurements by polarized diffuse Galactic dust emission. The TE signal is then 1.7 ± 0.5 and $0.5 \pm 0.3\ \mu\mathrm{K}^2_{\mathrm{CMB}}$ for $|b| \geq 5$ and 10 deg respectively. The upper limit on E and B mode polarization becomes $0.2\ \mu\mathrm{K}^2_{\mathrm{CMB}}$ (2σ). If the physical properties of dust radiation on the fraction of the sky observed by Archeops are representative of the whole sky, and if the actual level of E and B mode polarization is close to this upper limit, then dust polarized radiation will be a major foreground for determining the polarization power spectra of the CMB at high frequencies above 100 GHz.

Key words. cosmology: cosmic microwave background – cosmology: observations – polarization – ISM: dust, extinction

⋆ Richard Gispert passed away few weeks after his return from the early mission to Trapani.

1. Introduction

The Cosmic Microwave Background (CMB) is now considered as one of the most sensitive probes to the physics of the early Universe. A great number of experiments have measured its temperature anisotropy power spectrum over a wide range of angular scales (for a review, see Wang et al. 2003) until WMAP recently gave a cosmic variance limited estimate up to the rise of the second acoustic peak (Bennett et al. 2003a).

CMB polarization provides a wealth of complementary information. First, it brings additional cosmological information that break degeneracies that remain in the determination of cosmological parameters with temperature anisotropy data alone (see e.g. Zaldarriaga et al. 1997). Perhaps more importantly, it sheds light directly on inflation through the B mode polarization that is generated only by primordial gravity waves produced during that era (Seljak & Zaldarriaga 1997; Kamionkowski et al. 1997). Distortions of the E modes by large scales structures weak lensing also induce a B_{WL} signal, distinguishable from the primordial B by its non-Gaussianity. This B_{WL} component in turn provides useful information about the dark matter distribution (e.g. Benabed et al. 2001) and the mass of neutrinos at the precision of 0.04 eV for an experiment e.g. 20 times more sensitive than Planck (Kaplinghat et al. 2003).

CMB polarization is however 2 to 5 orders of magnitude smaller than temperature anisotropies and therefore still remains to be accurately measured. It is now becoming accessible thanks to improved instrumental sensitivities. The first detection of the E modes has been reported by DASI (Kovac et al. 2002). This result has been confirmed by the same team (Leitch et al. 2005), CAPMAP (Barkats et al. 2005) and CBI (Readhead et al. 2004). WMAP has also provided an estimate of the TE correlation spectrum (Kogut et al. 2003) fully compatible with an inflationary scenario.

Instrumental sensitivity is not the only issue in the determination of the power spectrum of the polarized CMB anisotropies. Other astrophysical components also contribute to the sky brightness and polarization at the wavelengths of interest and must be subtracted. These *foregrounds*, mainly dominated by the emission of diffuse dust and by the radiation of extragalactic point sources, are often not well constrained or even not experimentally measured in the case of polarization.

Ground based experiments such as those mentioned above observe small regions of the sky. They can then choose them where foregrounds are weak and are less prone to contamination by Galactic emission. It is not the case for full sky experiments such as WMAP and Planck. At the Planck–HFI frequencies and for future bolometer experiments, the dominant component is the radiation from Galactic Interstellar Dust (ISD). The submillimetre and millimetre (hereafter submm) *intensity* of the ISD emission can be inferred from IRAS and COBE–DIRBE extrapolations (e.g. Finkbeiner et al. 1999, hereafter FDS) and has been measured on large scales by COBE–FIRAS (Reach et al. 1995; Boulanger et al. 1996; Lagache et al. 1998). However, little is known about ISD *polarization* emission on scales larger than 10 arcmin, i.e. those that are the most relevant for current CMB studies. Few models have been proposed (Prunet et al. 1998) that rely on specific hypothesis about the orientation of the alignment of the grains and the distribution of matter in dust clouds, due to lack of experimental data. Indeed, ground–based observations of submm ISD polarization are concentrated on high angular resolution (arcminute scale) star formation regions. Indirect evidence for large scale polarization comes from the polarization of starlight in extinction (Serkowski et al. 1975), but as reviewed by Goodman (1996), these measurements of background starlight polarization lead to ambiguous interpretation. In particular, the visible data are biased by low column density lines of sight and do not fairly sample more heavily reddened ones. Direct submm measurements are therefore highly required both for Galactic studies of the large scale coherence of the magnetic field and in the field of CMB polarization, but are rather challenging as they require sensitivities comparable to those of CMB studies.

Recently, Benoît et al. (2004a) have reported the first measurement of the submillimetre diffuse polarized emission by interstellar dust in the vicinity of the Galactic plane using the Archeops experiment. They show that the Galactic plane is significantly polarized at the 3−5% level and that dense clouds can be polarized up to 10% or more. This indicates that the dust intrinsic radiation is highly polarized and that the grain alignment mechanism is very effective. Considered with the possible large scale coherence of the polarization orientation, it shows that the dust polarized emission could be an important foreground for CMB polarization studies, especially on large angular scales.

Here, we wish to give a first answer to this question with the evaluation of the dust polarization power spectra away from the Galactic plane and in diffuse regions, on angular scales ranging from $\ell = 3$ to $\ell = 70$. Section 2 briefly introduces Archeops and its polarization capabilities. Section 3 presents the processing applied to the data and Sect. 4 describes the evaluation of the polarized angular power spectra. Section 5 presents our main results. We conclude in Sect. 6 with the extrapolation of our results to lower frequencies where the CMB dominates, to give an estimate of the dust contamination in the measurements of the CMB polarization power spectra.

2. The Archeops instrument

Archeops[1] is a balloon borne bolometer experiment that aimed at measuring the CMB temperature anisotropy over large and small angular scales. It provided the first determination of the C_ℓ spectrum from the COBE multipoles (Smoot et al. 1992) to the first acoustic peak (Benoît et al. 2003a) from which it gave a precise determination of the main cosmological parameters, such as the total density of the Universe and the baryon fraction (Benoît et al. 2003b). Archeops was also designed as a test bed for Planck-HFI and therefore shared the same technological design: a Gregorian off–axis telescope with a 1.5 m primary mirror, bolometers operating at common frequencies (143, 217, 353 and 545 GHz) cooled down at 100 mK by a ^{3}He/^{4}He dilution designed to work at zero gravity and similar scanning strategy. A detailed description of the instrument

[1] http://www.archeops.org

and its performances can be found in Benoît et al. (2002) and Benoît et al. (2003b).

At 353 GHz where dust thermal radiation is dominant, Archeops has 6 bolometers mounted in 3 Ortho Mode Transducer[2] (hereafter OMT) pairs that are sensitive to polarization in order to study the properties of the polarized dust diffuse radiation. The three OMTs are oriented at 60 degrees from each other to enable the full recovery of the Q and U Stokes parameters and to minimize the correlations in their determination. Archeops was launched on February 7th, 2002, from the CNES/Swedish facility of Esrange, near Kiruna (Sweden). The flight brought about 12 hours of high quality night data.

3. Data processing and map making

A detailed description of the data processing and the polarization map making is given in Benoît et al. (2003b) and Benoît et al. (2004a).

The main steps on the Archeops data processing are the following. First, the reconstruction of the pointing during flight, with rms error better than 1 arcmin (Bourrachot 2004), is performed using the data from a bore-sight mounted optical star sensor aligned to each photometer using Jupiter observations. Second, corrupted data (including glitches and bursts of noise) in the Time Ordered Information (TOI), representing less than 1.5%, are flagged and not considered in the following processing. Third, low frequency drifts on the data, generally correlated to house-keeping information (altitude, attitude, cryostat temperatures, the CMB dipole) are removed using the latter as templates. Fourth, high frequency decorrelation is performed in few chosen frequency intervals of ∼1 Hz width to remove non-stationary high-frequency noise. Fifth, the corrected timelines are then deconvolved from the bolometer time constant and the flagged corrupted data are replaced by a constrained realization of noise. Sixth, low frequency atmospheric residuals and noise are subtracted using a destriping procedure which preserves the sky signal to better than 2% on large angular scales (Bourrachot 2004). To improve the quality of the removal of atmospheric residuals we have also performed a component separation analysis in the time ordered data using the SMICA-MCMD algorithm (Delabrouille et al. 2003) over all the Archeops channels. From this analysis we have constructed a template of the atmospheric contribution to the Archeops data which has been fit and removed from each of 353 GHz bolometers preserving the dust emission to better than 5% (see Tristram et al. 2005b, for more details). Finally, a bandpass filtering between 0.033 and 38 Hz has been performed to reject high frequency noise and non physical components at lower frequencies than the payload spin frequency (∼2 rpm).

The six bolometers are cross-calibrated as discussed on Sect. 4.3.2. The absolute calibration is obtained from a correlation between the Galactic latitude profiles from FIRAS "dust spectrum" maps and those of Archeops. It has an absolute accuracy of about 12%. This affects only the absolute values

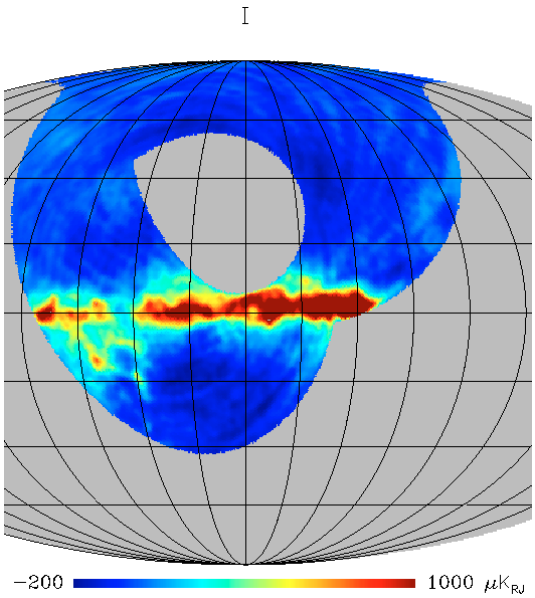

Fig. 1. Total unpolarized intensity I measured by Archeops at 353 GHz. Map centered on Galactic longitude $l = 120$ in Galactic coordinates. The pixel size is 27 arcmin smoothed by a 2 deg beam FWHM to match the 1.88 deg pixel size (HEALPix parameter $n_{\rm side} = 32$) used throughout the analysis. Grid lines are spaced by 20 deg.

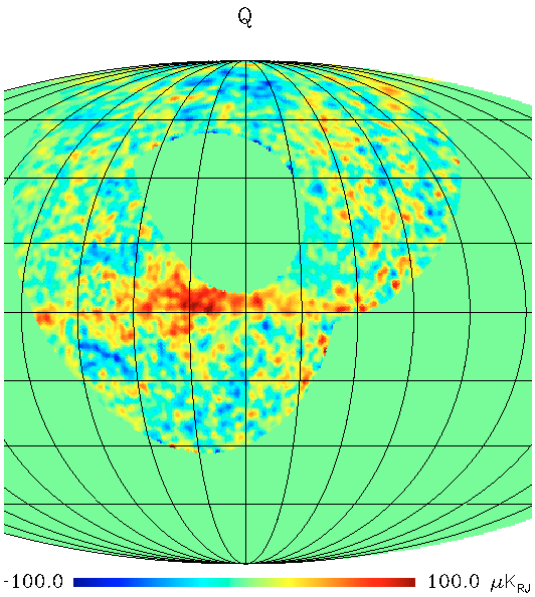

Fig. 2. Stokes parameter Q measured by Archeops at 353 GHz.

of I, Q, U but neither the degree of polarization nor its orientation. A detailed description of the calibration is given in Benoît et al. (2003b).

The data processed and calibrated as above have been projected into polarization maps using the algorithm described in Ponthieu 2003. The maps produced are shown in Figs. 1−3. A significant polarization level in the Galactic plane was first reported by Archeops (Benoît et al. 2004a) for regions with longitudes between 100 and 120 degrees and between 180 and 200 degrees. The new data processing allows us to reconstruct

[2] Planck-HFI has since changed for the Polarized Sensitive Bolometer (PSB) technology to measure polarization of radiation.

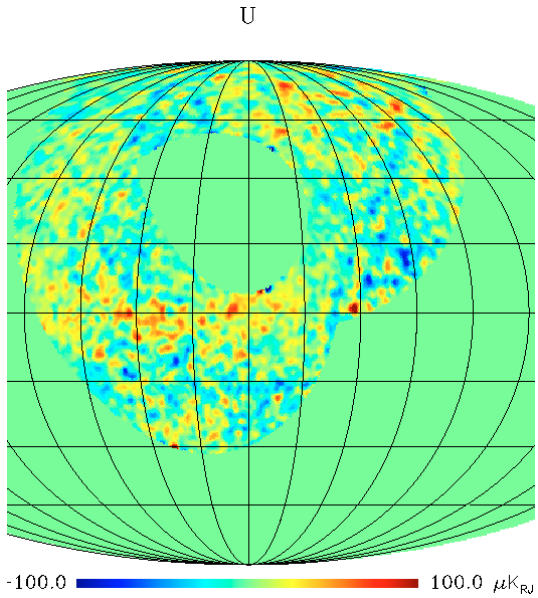

Fig. 3. Stokes parameter U measured by Archeops at 353 GHz.

polarization on all the Galactic plane observed by Archeops and to fill the gap between 120 and 180 degrees.

The noise correlation matrix on those maps have been computed using pure noise simulations which are described in Sect. 4.2.

4. Evaluation of the polarization power spectra

4.1. Formalism

For a direction of observation $\mathbf{n}$, we define the Stokes parameters I, Q and U in the tangential plane with respect to $(-\mathbf{e}_\theta, \mathbf{e}_\varphi)$. The angle of the polarization is oriented from the North Galactic pole through East to the South Galactic pole (counterclockwise).

For statistical analysis, the use of E and B (Seljak & Zaldarriaga 1997) is however more suitable because these quantities are scalar and independent of the coordinate system. We here estimate these quantities and the correlation between E and T using the method described in Chon et al. (2004). The spin-2 nature of Stokes parameters leads us to define

$$P \equiv Q + \mathrm{i}U. \tag{1}$$

When the polarized two point correlation functions are estimated in real space between two directions $\hat{n}_1$ and $\hat{n}_2$, one has to rotate P by angles α_1 and α_2 respectively to align the axes defining Q for each direction of observation with the geodesic connecting $\hat{n}_1$ and $\hat{n}_2$ such that

$$\overline{P}(\hat{n}_1) \equiv \mathrm{e}^{2\mathrm{i}\alpha_1} P(\hat{n}_1) \tag{2}$$
$$\overline{P}(\hat{n}_2) \equiv \mathrm{e}^{2\mathrm{i}\alpha_2} P(\hat{n}_2). \tag{3}$$

We then define the correlation functions

$$\xi_-(\theta) \equiv \langle \overline{P}(\hat{n}_1)\overline{P}(\hat{n}_2)\rangle = \sum_\ell \frac{2\ell+1}{4\pi}(C_\ell^{EE} - C_\ell^{BB})\, d^\ell_{2-2}(\theta)\,, \tag{4}$$

$$\xi_+(\theta) \equiv \langle \overline{P}^*(\hat{n}_1)\overline{P}(\hat{n}_2)\rangle = \sum_\ell \frac{2\ell+1}{4\pi}(C_\ell^{EE} + C_\ell^{BB})\, d^\ell_{22}(\theta)\,, \tag{5}$$

$$\xi_\times(\theta) \equiv \langle T(\hat{n}_1)\overline{P}(\hat{n}_2)\rangle = \sum_\ell \frac{2\ell+1}{4\pi} C_\ell^{TE}\, d^\ell_{20}(\theta)\,, \tag{6}$$

where $\hat{n}_1 \cdot \hat{n}_2 = \cos\theta$ and $d^l_{mm'}$ are the reduced Wigner D-matrices. The C_ℓs angular power spectra are then obtained by the following integration:

$$C_\ell^{EE} - C_\ell^B - 2iC_\ell^{EB} = 2\pi \int_{-1}^{1} \hat{\xi}_-(\theta) d^\ell_{2-2}(\theta) \mathrm{d}\cos\theta, \tag{7}$$

$$C_\ell^{EE} + C_\ell^B = 2\pi \int_{-1}^{1} \hat{\xi}_+(\theta) d^\ell_{22}(\theta) \mathrm{d}\cos\theta, \tag{8}$$

$$C_\ell^{TE} + iC_\ell^{TB} = 2\pi \int_{-1}^{1} \hat{\xi}_\times(\theta) d^\ell_{20} \mathrm{d}\cos\theta. \tag{9}$$

We estimate those quantities with the software SpicePol (Chon et al. 2004) that uses the HEALPix package (Gorski et al. 1998) to compute the pseudo-C_ℓs from the raw maps: $\tilde{C}_\ell^{TE}$, $\tilde{C}_\ell^{EE}$, $\tilde{C}_\ell^{BB}$, from which we obtain an estimate of the signal plus noise angular power spectra. The noise contribution is estimated through Monte-Carlo simulations (Sect. 4.2) and subtracted, producing estimates of the angular polarized power spectra. Because of approximations used by SpicePol it can not produce estimates of $\tilde{C}_\ell^{TB}$ and $\tilde{C}_\ell^{EB}$. The noise variance of the estimated power spectra is then given by:

$$\sigma^2(C_\ell^{XX}) = \frac{2}{(2l+1)f_{\mathrm{sky}}} \quad N_\ell^{XX\,2} \tag{10}$$

$$\sigma^2(C_\ell^{TE}) = \frac{1}{(2l+1)f_{\mathrm{sky}}} \left[N_\ell^{TE\,2} + N_\ell^{TT} C_\ell^{EE} + N_\ell^{EE} C_\ell^{TT} + N_\ell^{TT} N_\ell^{EE}\right] \tag{11}$$

where X stands for T, E or B, N is the noise and f_{sky} is the fraction of the sky taken for the analysis. The total uncertainty on the determination of a power spectrum includes both the variance of the noise and the variance of the signal itself. The CMB has known statistics properties (Gaussian, at least to the first order) and so, the sample variance can be accounted for analytically. It is not the case for Galactic dust whose statistics on large angular scales, especially regarding polarization, is poorly know. We therefore choose not to include any sample variance estimation in the error bars. However, to address the generalization of our results obtained on 20% of the sky to the whole sky, we have computed the TT angular power spectrum using the FDS template, both on the whole sky and on the Archeops sky coverage. We find a 25% difference. Assuming that polarization follows the same trend, a similar sample variance can be quoted.

The dominant term in Eq. (11) is the product of the covariance of temperature by the polarization noise $N_\ell^{EE} C_\ell^{TT}$. These relations are however only handy approximations to the true uncertainties and need an empirical adjustment of the f_{sky} parameter that is performed using the simulations described in

Sect. 4.2. These simulations are also used to compute the noise power spectra.

The temperature power spectrum C_ℓ^{TT} and its error bars are computed using the Xspect method (Tristram et al. 2005a) which uses 15 cross power spectra from the six detectors and no auto power spectrum in order to avoid corrections induced by the detector noise.

4.2. Instrumental noise

The noise power spectrum of the bolometers is estimated from a four step process already applied in Benoît et al. (2003a) in the context of the C_ℓ^{TT} evaluation. First, the Galactic plane region is masked and interpolated in the time domain with slowly varying functions. Secondly, these timelines are projected onto maps that are deprojected to obtain a second timeline with a higher signal to noise ratio. We then subtract this second timeline from the original one to obtain a noise dominated timeline and compute its time domain power spectrum. Simulations including realistic noise and Galactic contamination show that this process allows the recovery of the true noise power spectrum at the 5% level.

From these time domain noise power spectra, we generate noise timelines for the six polarized bolometers and project them onto maps in the same way as the real data. The same statistical analysis as the one applied to the data is performed on 250 of such noise maps to have a good estimate of the noise angular power spectra. These power spectra are then subtracted from the Archeops polarized angular power spectra in order to correct them from the noise bias. Finally, we compute the uncertainties on the polarization power spectra using Eqs. (10) and (11).

4.3. Systematic effects

Three main sources of systematic effects are likely to affect the evaluation of the polarization correlations: the filtering applied to the data, the uncertainty on the cross-calibration between the detectors and the uncertainty on the knowledge of the exact orientation of the polarizers on the focal plane. We address these three issues separately.

4.3.1. Filtering

The lower frequency bound of the applied bandpass filtering is 0.033 Hz, which corresponds to the first harmonic $f_{\rm spin}$ of the rotation of the gondola (2 rpm). Because of the spinning of the instrument, few physical components at frequencies below $f_{\rm spin}$ in the timeline are projected on the map. The high pass therefore ensures that no physically irrelevant and dipole-like components remain in the timelines. A low pass filtering is then applied to the timelines at 38 Hz to remove high frequency noise. To correct from this effect on the angular power spectra we have computed an effective filtering function F_ℓ in the multipole space from simulations of temperature Gaussian fields with a flat power spectrum. The maximum correction is at low ℓ and is less than 2%.

We have also checked that the filtering did not induce any spurious polarization such as leaks from total intensity into polarization. For this we have applied the bandpass filter to simulated timelines, deprojected from the FDS template at 353 GHz, for the six bolometers involved in the determination of the angular power spectra. Then, we have reconstructed I, Q and U maps for which we have extracted the temperature and polarization power spectra. No spurious polarization was produced at the level of 0.1%.

Finally, the destriping and component separation processes have shown to filter out 5% of the data at most (Tristram et al. 2005b).

4.3.2. Cross calibration

Stokes parameters are mainly estimated from the differences of the outputs of bolometers that measure orthogonal polarization states. An error in the cross calibration between detectors generates a systematic leak of total intensity into polarization. The cross calibration of Archeops channels is described in details in Benoît et al. (2004a) and relies on the scaling of Galactic intensity profiles computed from each bolometer. The cross calibration coefficients are then determined at the 2% level. In order to give a conservative upper limit to the effect of this uncertainty on the angular power spectra, we forced the cross calibration coefficients to values which deviate by 2% and maximized the relative difference between two orthogonal photometers. The angular power spectra were then estimated with this new set of coefficients and the error bars were derived from the standard deviation of 200 simulations, assuming a symmetric uncertainty. This uncertainty is about 5% of the statistical error bars.

4.3.3. Polarizer relative orientation

The accurate positioning of the polarizers in the focal plane is made difficult by the complexity of the instrument. We therefore checked that they were correctly placed during the preflight ground calibrations and found that they were indeed in their nominal configuration with a 1σ uncertainty of 3 degrees. A mismatch between the assumed and the real orientations of the polarizers generates a relative error of a few percents on the reconstructed Stokes parameters (Kaplan et al. 2001). In order to estimate the error induced by the uncertainty of the knowledge of the accurate positionning of the polarizers, we have performed simulations in which these angles are forced to random values different from those used for the I, Q, U reconstruction. The resulting uncertainty is of the same order as that of the cross calibration uncertainty, that is to say about 5% of the statistical error bars.

5. Results

We estimate the angular power spectra as a function of cuts of the data in Galactic latitude in order to remove the effects of regions with the strongest dust emission along the Galactic plane. Figure 4 gives the power spectra for $|b| \geq 5$, $|b| \geq 10$, and $|b| \geq 20$. The spectrum for C_ℓ^{TT} oscillates as a function

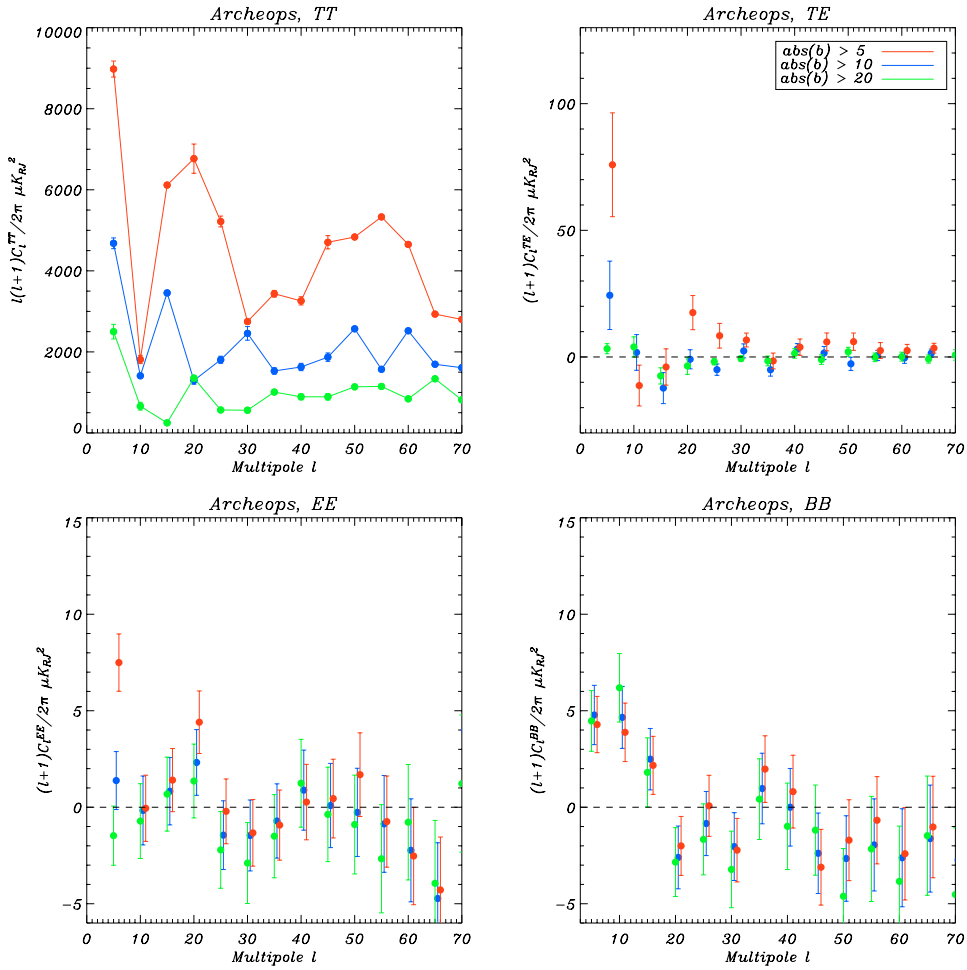

Fig. 4. Clockwise from top left: power spectra C_ℓ^{TT}, C_ℓ^{TE}, C_ℓ^{BB} and C_ℓ^{EE} computed from the 353 GHz Archeops data for three different Galactic cuts $|b| \geq 5$, 10, and 20 deg. At low ℓ the power in C_ℓ^{TT}, C_ℓ^{TE}, and C_ℓ^{EE} decreases with increasing $|b|$, as would be expected from a Galactic signal. Since the power in C_ℓ^{BB} does not change with $|b|$ its source is probably not astrophysical. ASCII files of these data can be obtained at `http://www.archeops.org/info_polar.html`.

of ℓ, with the amplitude of oscillation increasing with decreasing ℓ. These features are consistent with a Galactic origin for the signal as discussed in Sect. 5.1.1.

Since the Archeops data probe the dust diffuse emission and not local clouds in the Galactic plane it is likely that the orientation and coherence of the magnetic field is similar for latitudes larger than 5 and larger than 10 deg. Therefore, the more dust there is along the line of sight, the more intense the emission should be, and the more power we expect in the temperature and polarization spectra. According to these arguments there should be a monotonic decrease of power in the spectra with increasing latitude cuts, as observed for the TT, TE and EE data.

The *TE* Spectrum: on large angular scales $3 \leq \ell \leq 8$ there is a $\sim 4\sigma$ detection for $|b| \geq 5$ with a magntidue of $(\ell + 1)C_\ell^{TE}/2\pi = 76 \pm 21\ \mu\mathrm{K}_{\mathrm{RJ}}^2$ and a $\sim 2\sigma$ detection for $|b| \geq 10$ with a magnitude of $(\ell + 1)C_\ell^{TE}/2\pi = 24 \pm 13\ \mu\mathrm{K}_{\mathrm{RJ}}^2$. For $|b| \geq 5$ there is also a $\sim 2\ \sigma$ detection for $18 \leq \ell \leq 23$, corresponding to a peak in the temperature spectrum at the same ℓ bin.

The *EE* Spectrum: on large angular scales $3 \leq \ell \leq 8$ there is a $\sim 5\sigma$ detection for $|b| \geq 5$ with a magnitude of $(\ell + 1)C_\ell^{EE}/2\pi = 7.5 \pm 1.5\ \mu\mathrm{K}_{\mathrm{RJ}}^2$ and a $\sim 2\sigma$ for $18 \leq \ell \leq 23$. Otherwise, the power in the EE spectra is consistent with zero for all ℓ's for $|b| \geq 10$ and for $|b| \geq 20$ and at $20 \leq \ell \leq 70$ for all latitude cuts. Similar to the TE spectrum, the power measured for EE on all scales decreases with increasing latitude, which is consistent with a Galactic origin for the signal.

The *BB* Spectrum: there are detections of power in the first few ℓ bins and the spectrum is consistent with no power for $\ell \geq 19$. The power at the low ℓ bins does not depend on Galactic latitude cut. We argue below that models of polarization from dust emission predict a decrease of power in both the EE and BB spectra with Galactic latitude cut and therefore the BB signal at low ℓ is probably spurious. Unlike the CMB for which E and B have different physical sources, dust is expected to produce comparable amounts of E and B. A difference is however expected on large angular scales since the observed coherence of the polarization orthogonal to the Galactic plane leads to a stronger E signal. However, since we have no physical model to explain the constant amplitude of BB on our first bins, we think it is caused by an unknown systematic effect. This effect should affect EE and BB by the same amount so we chose to provide a common upper limit at $(\ell + 1)C_\ell^{EE,BB}/2\pi < 11\ \mu\mathrm{K}_{\mathrm{RJ}}^2$

at 353 GHz for $|b| \geq 5$. This effect is less likely to affect TE since the signal to noise is then much higher.

5.1. Comparison with models

In this section we compare our results to models of diffuse Galactic dust emission. First, we compare the TT power spectrum to those expected using a Galactic cosecant-law model and using the FDS model. Second, we obtain an alternative estimate of the TE spectrum by cross-correlating the FDS template with the Archeops Q and U maps. Finally, we compare the measured spectra to those calculated on the basis of a simplified physical model of polarized emission from dust.

5.1.1. Pure cosecant-law Galactic emission

Due to the disk geometry of the Galaxy, the integrated emission along a given line of sight increases as the absolute value of the latitude decreases. This is well approximated by a cosecant law of the form $I(b) \propto 1/\sin(b)$. When this Galactic contribution is subtracted, the angular power spectrum of the remaining diffuse dust has the form $C_\ell \propto \ell^{-3}$ (Gautier et al. 1992; Wright 1998).

We choose to leave the Galactic contribution in our data such that we can assess its magnitude and its potential contamination of CMB polarization experiments (see Sect. 6). In order to estimate the influence of a cosecant law component in our data, we simulate such an emission analytically and with an amplitude compatible with the FDS template. The results are presented in Fig. 5 where we plot the TT angular power spectrum at different Galactic latitude cuts for the Archeops data, for the cosecant-law model and for the FDS template. There is a qualitative agreement between the oscillation pattern of the Archeops data for low Galactic latitude cuts and the pattern present for the cosecant-law model and for the FDS template. The agreement suggests that the cosecant-law emission dominates the observed Galactic dust emission at large angular scales.

5.1.2. *FDS*-Archeops correlation

It is interesting to correlate the Archeops Q and U data with available dust intensity maps. We quantify the correlation by calculating the cross-spectrum between the two data sets. This idea has already been succesfully applied to temperature anisotropy data sets (Abroe et al. 2004; Tristram et al. 2005b). For dust intensity we use the FDS template, based on IRAS 100 μm maps and extrapolated to 353 GHz ("model number 8") (Finkbeiner et al. 1999). We found that this model fits the Archeops temperature data at 353 GHz with fractional deviations of less than 20%. Figure 6 shows that the "FDS × Archeops" cross-spectrum (in blue) and the "Archeops × Archeops" TE power spectrum (in red) are consistent within the error bars. This result provides additional confidence that the detection of power in the Archeops × Archeops TE spectrum at low ℓ is due to polarized dust and is not spurious. We note that the cross-spectrum with the FDS map avoids correlated noise that is inherent in the Archeops × Archeops spectrum and thus the agreement between the two results suggests that correlated noise did not induce spurious results.

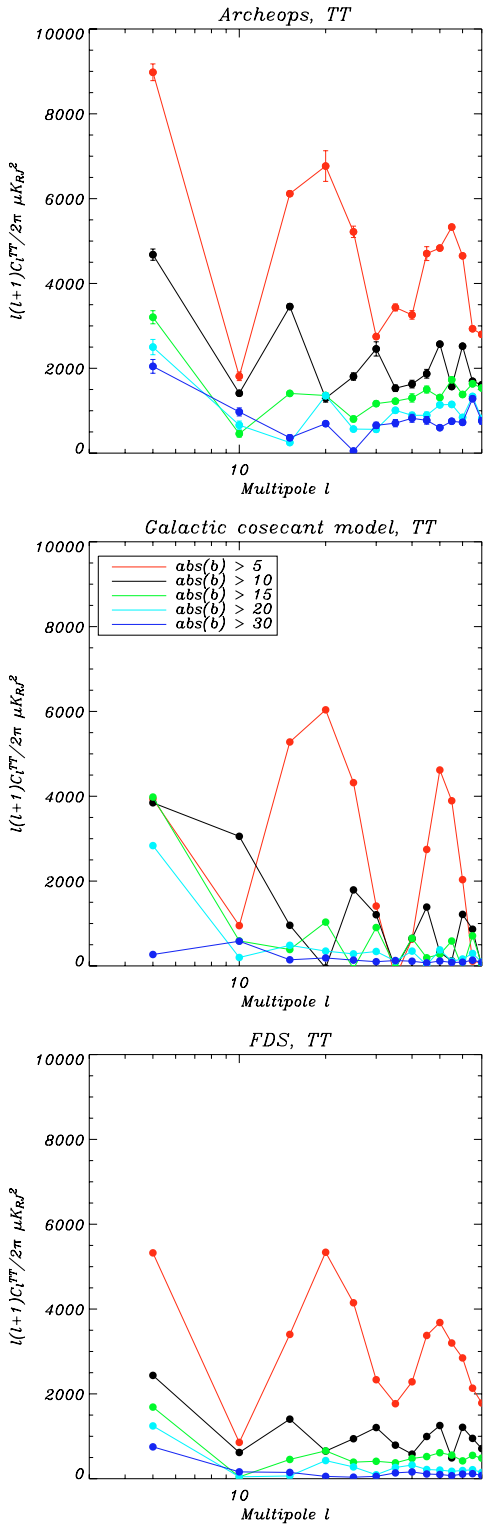

Fig. 5. Temperature angular power spectrum of Archeops data (*upper diagram*), of a pure Galactic cosecant emission law simulation (*middle diagram*) and of a FDS template (*lower diagram*) computed using Xspect for five different Galactic cuts.

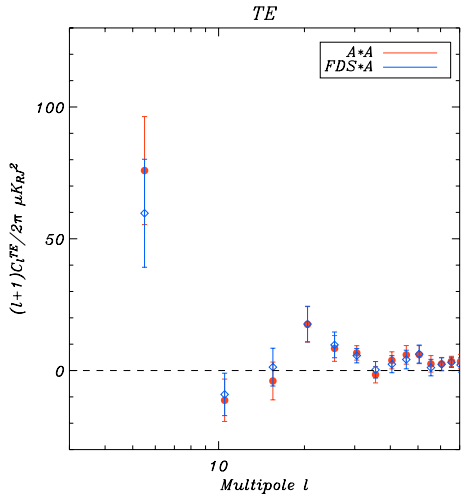

Fig. 6. TE angular power spectra for $|b| \geq 5$ either with Archeops data alone (red, circles) or with Archeops Q and U data and I from the FDS template (blue, diamonds) on the Archeops region of observation extrapolated to 353 GHz (Finkbeiner et al. 1999).

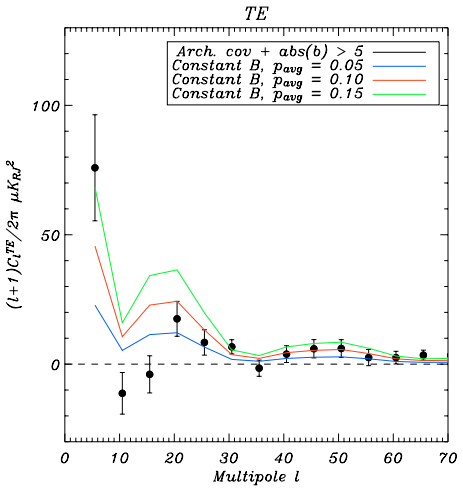

Fig. 7. Comparison between Archeops polarized angular power spectra and those of a simple model of the Galactic magnetic field for all latitudes $|b| \geq 5$. The large scale magnetic field is assumed to be constant and oriented along the local spiral arm. Dust is assumed to be aligned orthogonaly to it. The effective degree of alignment of the grains together with the dust intrinsic polarized emissivitiy is assumed to lead to 5 (blue), 10 (red) and 15% (green) effective degree of polarization.

5.1.3. Comparison to a simple physical model of Galactic dust polarization

In a given direction of observation, the measured Stokes parameters are the result of the integral along the line of sight of the local Stokes parameters. These, in turn, depend on the local alignment of dust grains with the magnetic field and on the intrinsic degree of polarization. Precise modelling of the diffuse emission due to dust and its polarized angular power spectra is a complex problem. Previous work has shown that on large scales, the alignement of dust grains was compatible with a Galactic magnetic field aligned with the spiral arms (Fosalba et al. 2002; Benoît et al. 2004a, and references therein). However, such work relate to data at low Galactic latitudes $|b| \leq 10$ deg, and the extrapolation at higher latitudes yet remains uncertain due to lack of data. We here use a toy model of extrapolation at high latitudes of these polarization properties that gives qualitative agreement with the Archeops data.

Since we are here looking at latitudes away from the Galactic plane, most of the dust that is being probed is in our vicinity. Typically, if we take the Galactic disk to be 200 pc thick, a line of sight at $b = 5$ deg exits the plane at ∼1.1 kpc from the observer. This is small compared to the size of the spiral arm in which we are located, and we therefore assume that the large scale magnetic field component aligned with the local spiral arm is along a constant direction on this portion of space. A realistic model would of course consider turbulence, but we are only interested here in a first order approximation. Based on Benoît et al. (2004a) who showed that dust diffuse emission in the vicinity of the Galactic plane was polarized at the 5% level, and that some dense clouds were polarized at more than 10%, we present in Figs. 7−9 results with three assumptions for the level of polarization of Galactic dust: $p(x) = 5, 10$, and 15%. We have only considered latitude cuts of $|b| \geq 5$ deg. Given the simplicity of the model, the relative agreement between the data and the shape and amplitude of the models is encouraging.

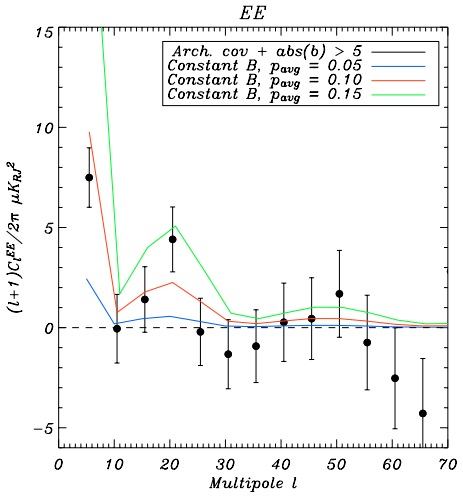

Fig. 8. Same as Fig. 7 for the EE angular power spectrum.

6. Dust contamination in CMB polarization estimates

Our results can be used to estimate the contamination of dust to CMB polarized angular power spectra. For this we need to extrapolate our measurements at 353 GHz to lower frequencies where the CMB is usually measured since it is where it is more intense.

Note that this extrapolation concerns large dust grains only. It does not take into account the so-called "anomalous emission", since (1) the latter does not contribute significantly at 353 GHz and (2) it is likely not to be polarized (e.g. Lazarian & Prunet 2001). Dust thermal radiation is the dominant foreground at frequencies above ≃90 GHz. At high frequencies it has long been described by a single grey body at a temperature of 17.5 K with a ν^2 emissivity (Boulanger et al. 1996).

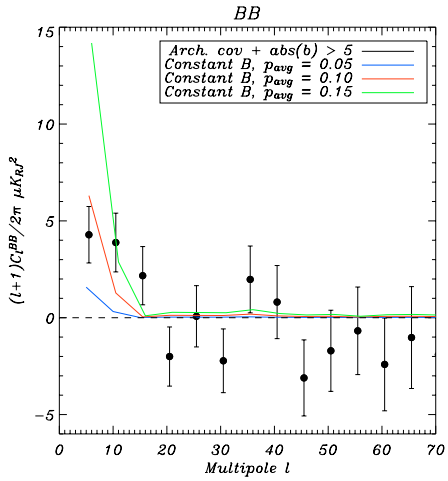

Fig. 9. Same as Fig. 7 for the *BB* angular power spectrum.

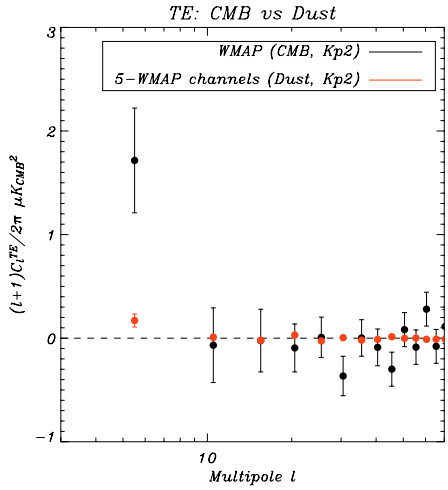

Fig. 10. Dust TE angular power spectrum in CMB temperature units as measured by Archeops at 353 GHz on the intersection of WMAP's Kp2 mask and the Archeops sky coverage, extrapolated down to the 5 WMAP frequency bands 23, 33, 41, 61 and 94 GHz (red) with a constant spectral index of 1.7 and averaged with an equal weight for each frequency (see Sect. 6 for details). WMAP's data (first year results) have been rebinned to match Archeops binning.

At low frequencies (∼300 to ∼100 GHz), the spectrum is not well constrained due to the lack of accurate measurements. We need to use the FIRAS and WMAP data jointly. The FIRAS data are used to compute the intensity value at 353 GHz and the WMAP data give the intensity value at 94 GHz. This then allows to derive the dust radiation spectral index.

To determine these dust intensities we use the method described in Lagache (2003) and derive the spectrum of the dust whose emission is correlated with the HI gas, using FIRAS and WMAP data in the Archeops region. We obtain a ratio $I_\nu(353)/I_\nu(94) = 134$ corresponding to a spectral index of 1.7 that we use in the following. Note that this value is very stable when different (large) regions of the sky are averaged. This is also the same value as the one obtained by Finkbeiner et al. (1999) in this frequency range (see discussion in Finkbeiner 2004). Using this spectral index of 1.7, we find for the largest angular scales ($3 \leq \ell \leq 8$), $(\ell+1)C_\ell^{TE}/2\pi = 1.7 \pm 0.5$ and 0.5 ± 0.3 $\mu\mathrm{K}^2_{\mathrm{CMB}}$ for $|b| \geq 5$ and 10 deg respectively at 100 GHz.

These results suggest that dust may be a very significant foreground for measurements of the CMB polarization angular power spectra, particularly if they include Galactic latitudes below $|b| < 10$ degrees. However, these measurements must be interpreted with care when considering the entire sky. Our data includes only 20% of the sky and generalization to the entire sky is questionable because of the complexity of the statistical properties of dust.

It is interesting to consider the relation between our results and those of the WMAP team. By combining data from *five* frequency bands at *lower frequencies* (23, 33, 41, 61 and 94 GHz) and for *the entire sky* the WMAP team has computed a value for the TE spectrum at $3 \leq \ell \leq 8$ of 1.72 ± 0.50 $\mu\mathrm{K}^2_{\mathrm{CMB}}$. Accurate extrapolation of the Archeops results into the WMAP data is complicated and is beyond the scope of this paper. (For example, it would require a detailed knowledge of the component separation methods, the relative weighting of the frequency bands and the shape of the beam.) However, it is easy to *illustrate* that combining data at lower frequencies reduces the effects of dust substantially. We extrapolate our results to the WMAP frequency bands with a constant emissivity spectral index of 1.7 in antenna temperature. We use an equal weight per frequency and use only the area of the sky that overlaps the Archeops data and WMAP's Kp2 mask. The result of this extrapolation is presented in Fig. 10. On scales of $3 \leq \ell \leq 8$ we find $(\ell+1)C_\ell^{TE}/2\pi = 0.17 \pm 0.06$ $\mu\mathrm{K}^2_{\mathrm{CMB}}$, which is about a factor of 10 smaller than both our estimate at 100 GHz, and WMAP's reported result.

When extrapolated to 100 GHz the upper limits that we found on the E and B modes for $|b| \geq 5$ become 0.2 $\mu\mathrm{K}^2_{\mathrm{CMB}}$. We note that the CMB B mode polarization is expected to be at most $\sim 10^{-3}$ $\mu\mathrm{K}^2_{\mathrm{CMB}}$ at $\ell \simeq 5$, if the reionization optical depth is as high as $\tau = 0.17$ (Spergel et al. 2003) and if the tensor to scalar ratio T/S is the highest compatible with current CMB temperature anisotropy measurements. If the actual level of polarized dust over most of the sky is close to the upper limit we found in this work then a subtraction of a large foreground signal will be necessary even at 100 GHz in order to detect the primordial gravitational waves on large angular scales.

7. Conclusions

In this paper we have presented the first measurements of the angular power spectra of the Galactic dust polarized diffuse emission on approximately 20% of the sky at 353 GHz by Archeops. On angular scales $3 \leq \ell \leq 8$, we obtain a 4 σ detection of $(\ell+1)C_\ell^{TE}(\mathrm{dust})/2\pi = 76 \pm 21$ $\mu\mathrm{K}^2_{\mathrm{RJ}}$ for $|b| \geq 5$ deg. On the same angular scales and for $|b| \geq 10$, we have a 2σ detection $(\ell+1)C_\ell^{TE}(\mathrm{dust})/2\pi = 24 \pm 13$ $\mu\mathrm{K}^2_{\mathrm{RJ}}$. This decrease in power is expected from the cosecant behaviour of the large scale component of the total intensity, which is shown to dominate the total intensity angular power spectrum. These results have been confirmed by using a template of the Galactic dust intensity from Finkbeiner et al. (1999) in place of the Archeops total intensity map to compute the TE angular power spectrum.

This spectrum agrees with the one derived from Archeops data alone on all angular scales within 1σ.

On the same sky coverage and for all angular scales $3 \leq \ell \leq 70$, we set upper limits to the E and B polarization at $(\ell + 1)C_\ell^{EE,BB}(\mathrm{dust})/2\pi \leq 11\ \mu\mathrm{K}^2_{\mathrm{RJ}}$.

Furthermore, the high degree of polarization seen in the Galactic plane by Benoît et al. (2004a) together with a simple model of the Galactic magnetic field and the alignment of dust grains, leads to estimates that are compatible with the data.

To estimate the contribution of Galactic dust to the measurement of polarized CMB anisotropies, we have extrapolated our results to the reference frequency 100 GHz, using a spectral index of 1.7, derived from FIRAS and WMAP data on the Archeops sky coverage. The TE modes becomes $(\ell + 1)C_\ell^{TE}(\mathrm{dust})/2\pi = 1.7 \pm 0.5$ and $0.5 \pm 0.3\ \mu\mathrm{K}^2_{\mathrm{CMB}}$ on $3 \leq \ell \leq 8$ for $|b| \geq 5$ and 10 deg respectively. The upper limit on the E and B modes becomes $0.2\ \mu\mathrm{K}^2_{\mathrm{CMB}}$. These values show that even at 100 GHz where dust radiation is expected to be lower than the CMB, its polarization may be very significant compared to the CMB and should be subtracted with care from the observations.

The effects of the polarization of dust are less severe at low frequencies. When extrapolating our measurements at 353 GHz to 20 GHz with the constant spectral index 1.7 and weighting the 5 WMAP frequencies equally we find a level of $(\ell + 1)C_\ell^{TE}(\mathrm{dust})/2\pi = 0.17 \pm 0.06\ \mu\mathrm{K}^2_{\mathrm{CMB}}$ for $3 \leq \ell \leq 8$ on the intersection between WMAP's Kp2 mask and Archeops sky coverage. This is about a factor of 10 smaller then the TE detection reported by the WMAP team for these angular scales.

The high level of polarization measured at 353 GHz by Archeops and anticipated at the reference frequency of 100 GHz, together with the uncertainties on dust spectral index and the extrapolation of its statistical properties to the whole sky call for further precise studies in order to subtract it precisely from CMB data. This is even more critical for the detection of the imprint of the primordial gravitational waves on the CMB B modes, that is expected to be much smaller than the present upper limit on dust B polarization.

Acknowledgements. We would like to pay tribute to the memory of Pierre Faucon who led the CNES team on this successful flight. The HEALPix package was used throughout the data analysis Gorski et al. (1998). We also thank A. Starobinsky for fruitful discussions.

References

Abroe, M. E., Borrill, J., Ferreira, P. G., et al. 2004, ApJ, 605, 607-613
Barkats, D., Bischoff, C., Farese, P., et al. 2005, ApJS, 159, 1
Benabed, K., Bernardeau, F., & van Waerbeke, L. 2001, Phys. Rev. D, 63, 043501
Bennett, C. L., Hinshaw, G., Spergel, D. N, et al. 2003, ApJS, 148, 135H
Bennett, C. L., Hill, R. S., Hinshaw, G., et al. 2003, ApJS, 148, 97B
Benoît, A., Ade, P., Amblard, A., et al. 2002, Astropart. Phys., 17, 101
Benoît, A., Ade, P., Amblard, A., et al. 2003a, A&A, 399, L19
Benoît, A., Ade, P., Amblard, A., et al. 2003b, A&A, 399, L25
Benoît, A., Ade, P., Amblard, A., et al. 2004a, A&A, 424, 571
Benoît, A., Ade, P., Amblard, A., et al. 2004b, in preparation
Boulanger, F., Abergel, A., Bernard, J.-P., et al. 1996, A&A, 312, 256
Bourrachot, A. 2004, Ph.D. Thesis, Université Paris VII
Chon, G., Challinor, A., Prunet, S., Hivon, E., & Szapudi, I. 2004, MNRAS, 350, 914
Delabrouille, J., Cardoso, J. F., & Patanchon, G. 2003, MNRAS, 346, 1089
Fosalba, P., Lazarian, A., Prunet, S., & Tauber, J. A. 2002, ApJ, 564, 762
Gautier, T. N.I., Boulanger, F., Perault, M., & Puget, J. L. 1992, ApJ, 103, 1313
Goodman, A. A. 1996, in Proc. Polarimetry of the Interstellar Medium, ed. W. G. Roberge, & D. C. B. Whittet, ASP Conf. Ser., 97, 325
Gorski, K. M., Hivon, E., Wandelt, B. D., et al. 1998, Proceedings of the MPA/ESO Conferece on Evolution of Large-Scale Structure: from Recombination to Garching 2−7 August 1998; ed. A. J. Banday, R. K. Sheth, & L. Da Costa [arXiv:astro-ph/9812350], http://www.eso.org/science/healpix
Heiles, C. 1996, in Polarimetry of the Interstellar Medium, ed. W. G. Roberge, & D. C. B. Whittet (San Francisco:ASP), ASP Conf. Ser., 97, 457
Finkbeiner, D. P., Davis, M., & Schlegel, D. 1999, ApJ, 524, 867
Finkbeiner, D. P. 2004, ApJ, 614, 186
Kamionkowski, M., Kosowsky, A., & Stebbins, A. 1997, Phys. Rev. D, 55, 7368,
Kaplan, J., & Delabrouille, J. 2001, Proceedings of the Astrophysical Polarized Foregrounds, 6−12 October 2001, Bologna, Italy
Kaplinghat, M., Knox, L., & Song, Y.-S. 2003, Phys. Rev. Lett., 91, 241301
Kogut, A., Spergel, D. N., & Barnes, C. 2003, ApJS, 148, 161
Kovac, J., Leitch, E. M., Pryke, C., et al. 2002, Nature, 420, 772
Lagache, G., Abergel, A., Boulanger, F., & Puget, J. L. 1998, A&A, 333, 709
Lagache, G. 2003, A&A, 2003, 405, 813
Lazarian, A., & Prunet, S. 2001, Astrophysical Polarized Foregrounds, AIP Conf. proceedings, ed. S. Cecchini, S. Cortiglioni, R. Sault, & C. Sbarra
Leitch, E., Kovac, J., Halverson, N., et al. 2005, ApJ, 624, 10
Lesgourgues, J., Polarski, D., Prunet, S., & Starobinsky, A. 2000, A&A, 359, 414
Ponthieu, N. 2003, On behalf of Archeops collaboration, proceedings of the Workshop The Cosmic Microwave Background and its Polarization, Minneaolis, March 2003, New Astronomy Reviews, ed. S. Hanany, & K. Olive
Prunet, S., Sethi, S. K., Bouchet, F. R., & Miville-Deschenes, M. A. 1998, A&A, 339, 187
Reach, W. T., Dwek, E., Fixsen, D. J., et al. 1995, ApJ, 451, 188
Readhead, A., Myers, S., Pearson, T., et al. 2004, Science, 306, 836
Seljak, U., & Zaldarriaga, M. 1997, PRD 55, 1830
Serkowski, K., Mathewson, D. S., & Ford, V. L. 1975, ApJ, 196, 261
Smoot, G. F., Bennett, C. L., Kogut, et al. 1992, ApJ, 396, L1
Spergel, D. N., Verde, L., Peiris, H. V., et al. 2003, ApJS, 148, 175
Tristram, M., Macías-Pérez, J. F., Renault, C., & Santos, D. 2005a, MNRAS, 358, 833
Tristram, M., Patanchon, G., Macías-Pérez, J. F., et al. 2005b, A&A, 436, 785
Wang, X., Tegmark, M., Jain, B., & Zaldarriaga, M. 2003, Phys. Rev. D., 68, 123001
Wright, E. L. 1998, ApJ, 496, 1
Zaldarriaga, M., Spergel, D. N., & Seljak, U. 1997, ApJ, 488, 1